RSC Advances

PAPER

View Article Online
View Journal | View Issue



Cite this: *RSC Adv.*, 2025, **15**, 14058

# Influence of the charge of 1,3,5-triaza-7-phosphaadamantane-based ligands on the anticancer activity of organopalladium complexes†

Tommaso Lorenzon, [a] Maria Vescovo,[a] Michele Maiullari,[a] Giovanni Tonon, [b] Nuno Reis Conceição, [c] Sónia A. C. Carabineiro, [cd] Abdallah G. Mahmoud, [d] Martin C. Dietl, [e] Nicola Demitri, [f] Laura Orian, [a] Pablo A. Nogara, [g] Isabella Caligiuri,[h] Flavio Rizzolio, [ah] A. Stephen K. Hashmi, [ei] Fabiano Visentin [b] and Thomas Scattolin *[a]

In this study, we report the synthesis and characterization of novel organopalladium complexes featuring 1,3,5-triaza-7-phosphaadamantane (PTA)-based ligands, including several cationic derivatives prepared as hexafluorophosphate salts to prevent halide exchange reactions. The complexes incorporate diverse organopalladium fragments—Pd(II)-vinyl, Pd(II)-butadienyl, Pd(II)-allyl, Pd(II)-imidoyl, Pd(II)-aryl, and Pd(0)-alkene—many of which have recently shown promising antitumor activity. Most reactions proceeded rapidly at room temperature under aerobic conditions using non-anhydrous solvents. Biological evaluation against ovarian cancer (A2780), cisplatin-resistant ovarian cancer (A2780*cis*), triple-negative breast cancer (MDA-MB-231), glioblastoma (U87), and non-cancerous fibroblasts (MRC-5) revealed the remarkable cytotoxicity of the complexes, particularly those with Pd(II)-butadienyl, Pd(II)-aryl, and Pd(0)-alkene fragments. These compounds demonstrated activity comparable to or exceeding cisplatin, with some showing up to two orders of magnitude greater efficacy. Importantly, the complexes were highly selective for cancer cells, exhibiting minimal toxicity toward MRC-5 fibroblasts, unlike cisplatin. Complex **14b**, that contains a Pd(0)-alkene fragment and two $MePTA^+$ ligands, was the only one that exhibited excellent cytotoxicity across all cancer cell lines, including glioblastoma. These findings underscore the potential of PTA-based organopalladium complexes as selective anticancer agents, warranting further *in vitro* and *in vivo* studies, as well as mechanistic investigations.

Received 26th March 2025
Accepted 22nd April 2025

DOI: 10.1039/d5ra02119g

rsc.li/rsc-advances



## Introduction

1,3,5-Triaza-7-phosphaadamantane (PTA) has emerged as a pivotal ligand in the field of coordination chemistry due to its unique structural features, including its remarkable water solubility, and exceptional stability even under physiological conditions.[1–3] This organophosphorus compound presents a distinctive cage-like structure reminiscent of adamantane, which confers it significant thermal and oxidative stability. PTA acts as a monodentate ligand, coordinating to metal centers primarily through its phosphorus atom. PTA is a strong electron donor, which significantly enhances its ability to stabilize metal centers when forming complexes. Additionally, the spatial arrangement around the phosphorus atom in PTA provides a moderate steric bulk, which can influence the coordination environment and reactivity of the resulting metal complexes.[1–5]

This coordination capability allows PTA to form stable complexes with a broad array of metals, including transition metals.[1–13] The possibility to modify the electronic properties of PTA by introducing different substituents on the nitrogen atoms further enhances its versatility, enabling the fine-tuning

[a]*Dipartimento di Scienze Chimiche, Università degli Studi di Padova, Via Marzolo 1, 35131 Padova, Italy. E-mail: thomas.scattolin@unipd.it*
[b]*Dipartimento di Scienze Molecolari e Nanosistemi, Università Ca' Foscari, Campus Scientifico Via Torino 155, 30174 Venezia-Mestre, Italy*
[c]*Centro de Química Estrutural, Institute of Molecular Sciences, Instituto Superior Técnico, Universidade de Lisboa, Av. Rovisco Pais, 1049-001 Lisboa, Portugal*
[d]*LAQV-REQUIMTE, Department of Chemistry, NOVA School of Science and Technology, Universidade NOVA de Lisboa, 2829-516 Caparica, Portugal*
[e]*Organisch-Chemisches Institut, Heidelberg University, Im Neuenheimer Feld 270, 69120 Heidelberg, Germany*
[f]*Elettra-Sincrotrone Trieste, S.S. 14 Km 163.5 in Area Science Park, 34149 Basovizza, Trieste, Italy*
[g]*Departamento de Bioquímica e Biologia Molecular, Centro de Ciências Naturais e Exatas, Universidade Federal de Santa Maria, Santa Maria, RS, Brazil*
[h]*Pathology Unit, Centro di Riferimento Oncologico di Aviano (C.R.O.), IRCCS Via Franco Gallini 2, 33081, Aviano, Italy*
[i]*Chemistry Department, Faculty of Science, King Abdulaziz University, Jeddah 21589, Saudi Arabia*

† Electronic supplementary information (ESI) available. CCDC 2411281 and 2411282. For ESI and crystallographic data in CIF or other electronic format see DOI: https://doi.org/10.1039/d5ra02119g

of ligands for specific catalytic, biological or material applications.[14–20]

In the realm of medicinal chemistry, PTA metal complexes have shown significant potential, particularly in the development of new anticancer agents.[1–3] The stability and unique electronic properties of PTA allow for the formation of complexes with enhanced biological activity and reduced toxicity compared to traditional metal-based chemotherapeutic agents. For example, PTA-platinum complexes are being investigated as alternatives to conventional platinum-based drugs, offering improved efficacy and fewer side effects.[19,21,22] However, the most famous class of biologically active PTA complexes is the RAPTA (Ruthenium Arene PTA) family.[23–30] These compounds have been extensively investigated as promising antimetastatic agents, with RAPTA-C (featuring a cymene ligand) and RAPTA-T (featuring a toluene ligand) emerging as the leading candidates.[31–38] Their antimetastatic activity appears to be linked to their ability to form covalent bonds with key proteins within cancer cells.

Much less explored is the coordination chemistry of PTA in organopalladium compounds. These organometallic derivatives have shown promising antitumor activity, especially towards *in vitro*, *ex vivo*, and *in vivo* ovarian cancer models, with some compounds exhibiting reduced cytotoxicity against non-cancerous cells.[39–50]

Our group has recently reported the synthesis and antitumor activity of compounds containing various organopalladium fragments such as Pd(II)-allyl,[40,46] palladacyclopentadienyl,[45] Pd(II)-imidoyl,[47] Pd(II)-vinyl,[39] Pd(II)-butadienyl,[39] Pd(II)-aryl[49] and Pd(0)-alkene.[41]

In this work, we propose to utilize some of these promising organopalladium fragments as tools to evaluate the influence of the nature of the PTA-based ligand used on the antitumor activity of the resulting complexes. Specifically, we will compare the activity of complexes containing PTA with those of homologous complexes that contain cationic PTA derivatives (Fig. 1).

It is well known that the charge of a complex has important implications for its therapeutic activity. In principle, cationic complexes or those containing cationic groups (*e.g.*, ammonium or phosphonium substituents) tend to exhibit good cellular uptake and primary localization in the mitochondria, whereas anionic complexes exhibit reduced cellular uptake.[51–53]

Therefore, the use of cationic derivatives of PTA should significantly shift the localization of the complexes studied in this work towards mitochondria, even in the presence of organopalladium fragments that typically target DNA (*e.g.*, Pd(II)-aryl)[49] or promote cell death mechanisms other than apoptosis, such as ferroptosis (*e.g.*, Pd(II)-butadienyls).[39]

Among the cationic derivatives of PTA examined in this work, one exhibits a structure very similar to acetylcholine. This ligand preserves the main characteristics of this important biomolecule, in conjunction with a suitable coordination site for the metal.[19] Moreover, with the aim of studying these complexes as potential therapeutic agents against different types of cancer, including brain cancer, they could exploit organic cation transporters (OCTs) expressed in the blood–brain barrier (BBB) to cross from the blood to the central nervous system, thus acting as Trojan horses for biologically active organopalladium fragments.[54,55]

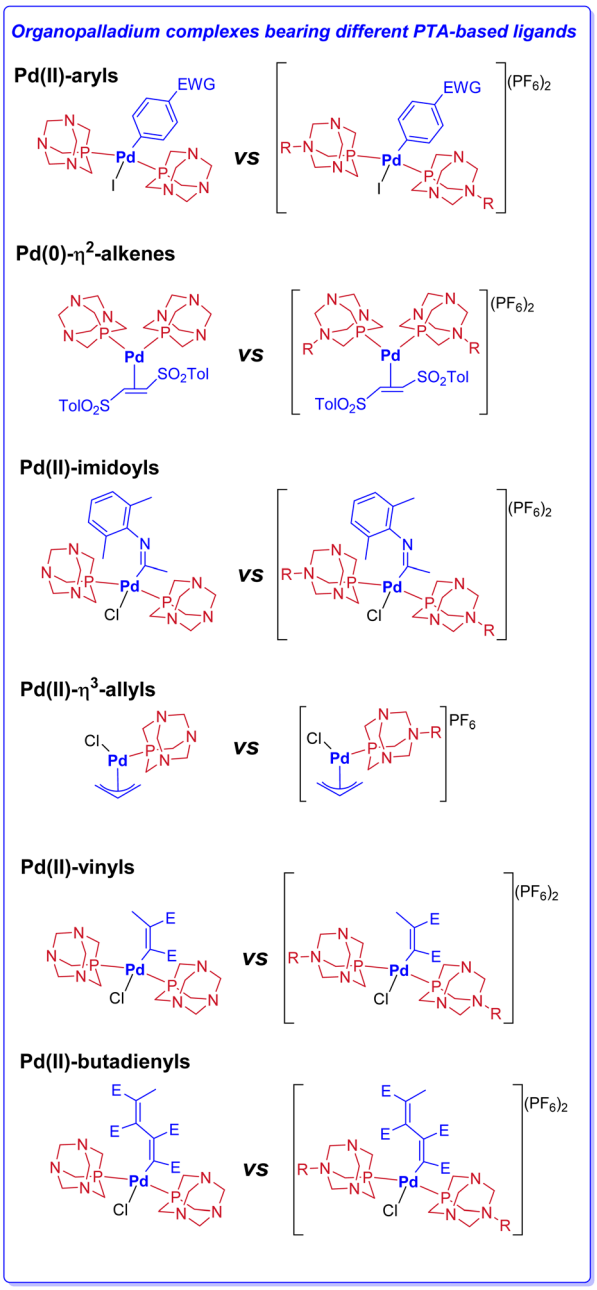


Fig. 1 Target complexes of this work.

## Results and discussion

### Synthesis of cationic PTA-based ligands

As stated in the introduction section, in addition to PTA (**a**), cationic PTA derivatives were also utilized as ligands in this work. Specifically, following procedures similar to those reported in the literature, the selective *N*-monoalkylation of PTA was performed with four different alkylating agents: (i) methyl iodide;[56] (ii) 2-bromoethyl acetate;[19] (iii) 4-(bromomethyl)benzoic acid;[57] and (iv) 5-(chloromethyl)-2-hydroxybenzaldehyde[57]

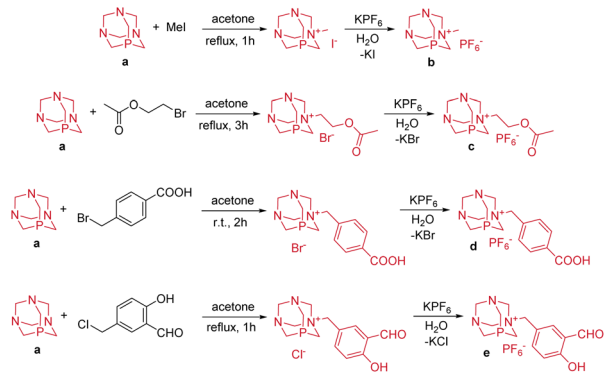


Scheme 1 Synthetic procedures to PTA-based ligands **b–e**.

(Scheme 1). The poor solubility of the obtained PTA ammonium salts in acetone allows for their easy isolation by simple filtration.

Compound **b** was chosen because it contains the simplest organic substituent (methyl group), thus representing the cationic version of PTA with the most comparable steric hindrance. Compound **c**, as previously mentioned, exhibits a structure very similar to acetylcholine, whereas derivatives **d** and **e** were selected because their copper and gold complexes have recently shown interesting catalytic and anticancer properties, respectively.[57,58]

To enable a proper comparison among the target organopalladium complexes, we decided to convert all the cationic PTA derivatives into their hexafluorophosphate congeners. This ensures that all final complexes contain the same non-coordinating counterion, therefore preventing potential halide exchange at the metal center.

This synthetic step proceeds quickly and with good yields, as the final products (**b–e**) precipitate from the aqueous solution containing $KPF_6$ and potassium halide (co-product).

The hexafluorophosphate PTA-based ligands (**b–e**) were thoroughly characterized by $^1$H and $^{31}$P NMR analyses.

Particularly diagnostic are the $^{31}$P NMR spectra, where a singlet can be observed between −80 and −87 ppm, which is markedly downfield shifted with respect to that of neutral PTA ($\delta \approx -102$ ppm). In addition, the diagnostic septet present at *ca.* −144 ppm indicates the presence of the hexafluorophosphate anion.

### Synthesis of Pd(II)-vinyl and Pd(II)-butadienyl complexes

Pd(II)-vinyl and Pd(II)-butadienyl complexes represent one of the most promising and emerging classes of organopalladium anticancer agents. These compounds exhibit high antitumor activity, particularly against ovarian cancer, often accompanied by low cytotoxicity towards non-cancerous cells.[39] Among the Pd(II)-vinyl and Pd(II)-butadienyl complexes recently studied by our group, the most promising ones contain two PTA ligands in a *trans* configuration (**3a** and **4a**). Detailed mechanistic studies on complex **4a** have shown that it induces cancer cell death through a ferroptotic mechanism, which is a decidedly unusual pathway among organopalladium anticancer compounds.[39] Moreover, this complex has demonstrated high efficacy against patient-derived high-grade serous ovarian cancer organoids as well as towards *in vivo* mouse models, with surprisingly low collateral toxicity even at high dosages.

Inspired by this recent contribution, we decided to synthesize a selection of new Pd(II)-vinyl and -butadienyl complexes bearing cationic PTA-based ligands. The procedure, which differs from the one previously proposed for using acetonitrile instead of dichloromethane, involves a direct reaction between the selected PTA-based ligand (**b–e**) and the palladium precursors **1–2**. These precursors bear the labile 2-methyl-6-(phenylthiomethyl)pyridine ligand and vinyl or butadienyl fragments, respectively (Scheme 2A and B). Acetonitrile was chosen as the solvent since it can dissolve both the phosphine ligands **b–e**, which are insoluble in dichloromethane, and the palladium precursors **1–2**.

All reactions reached completion within 30 minutes and the target complexes were fully characterized by NMR and elemental analysis.

The $^{31}$P NMR spectra of the products exhibit, in addition to the septet at *ca.* −144 ppm of the hexafluorophosphate anion, one singlet at *ca.* −40 ppm. This clearly indicates both the coordination of PTA-based ligands ($\Delta\delta \approx 40$ ppm with respect to the free ligand) and the mutual *trans* position of these ligands (the hypothetical *cis* isomer would generate two doublets).

The $^1$H NMR spectra confirm the nature of the obtained products, showing the methyl protons of the vinyl and butadienyl fragments (1.8–3.9 ppm), as well as signals of the methylene protons ($NCH_2N$ and $NCH_2P$) of the triazaphosphaadamantane moiety as multiplets between 4 and 5 ppm. Additionally, all characteristic signals of the alkyl substituents of the different PTA derivatives are present. Notably, all aforementioned signals exhibit chemical shifts different from those of the two starting reagents.

### Synthesis of Pd(II)-aryl and Pd(II)-allyl complexes

Pd(II)-aryl complexes is another interesting class of organopalladium compounds that has been recently investigated from a biological point of view. These organopalladium derivatives exhibit lower antiproliferative activity against cancer cells compared to their Pd(II)-vinyl or Pd(II)-butadienyl congeners[49] but, in a limited number of cases, they demonstrated good selectivity towards cancer cells over non-cancerous ones.

The primary biological target of neutral Pd(II)-aryl complexes appears to be DNA. In particular, for complexes bearing chelating diphosphine ligands, the interaction with the biological target and the consequent anticancer activity are closely related to the bite angle of the ancillary ligand. Specifically, smaller bite angles ensure higher DNA affinity and greater cytotoxicity of the compounds.[49]

Encouraged by these findings, we questioned whether it would be possible to expand the toolbox of neutral Pd(II)-aryl complexes by employing PTA in place of the classical triphenylphosphine, which was used in our recent study.[49] Moreover, with the final goal of evaluating the influence of complex charge on the biological properties of this class of compounds, we

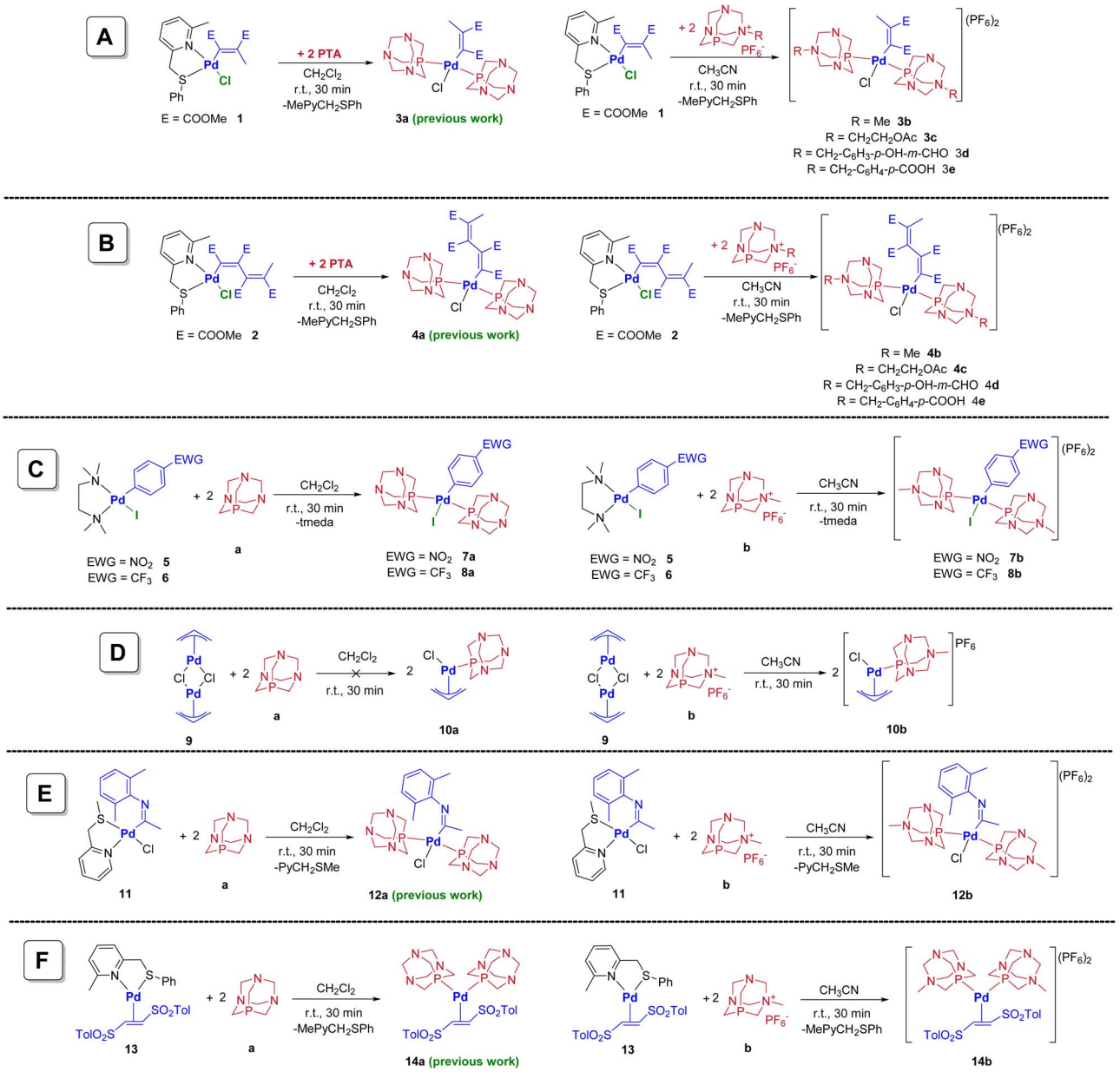


Scheme 2 Synthetic procedure to Pd(II)-vinyl (A), Pd(II)-butadienyl (B), Pd(II)-aryl (C), Pd(II)-allyl (D), Pd(II)-imidoyl (E) and Pd(0)-alkene (F) complexes.

selected [Me-PTA]$PF_6$ (**b**) as a cationic ligand to anchor to the Pd(II)-aryl fragment. Specifically, the complexes examined feature two PTA-based ligands, a 4-nitrophenyl or a 4-trifluoromethyl group, and one iodide ligand.

The reaction between Pd(II)-aryl precursors **5–6**, which contain the labile *N*,*N*,*N*′,*N*′-tetramethylethylenediamine (tmeda) ligand, and two equivalents of PTA (**a**) or [Me-PTA]$PF_6$ (**b**), yielded the target complexes **7a–b** and **8a** in good to excellent yields and purity. As usual, the reactions with the PTA ligand were carried out in dichloromethane, while those with the cationic [Me-PTA]$PF_6$ (**b**) derivative were performed in acetonitrile, systematically achieving completion within 30 minutes at room temperature (Scheme 2C and D). Notably, in the case of complex **8b**, some side-products difficult to eliminate were detected. For this reason, this complex was excluded from full characterization as well as from biological studies.

The new Pd(II)-aryl complexes **7a–b** and **8a–b** were fully characterized by NMR, XRD, and elemental analyses.

Taking the neutral complexes **7a** and **8a** as examples, the coordination of the PTA ligands and their mutual *trans* position can be confirmed by the presence of a singlet in the $^{31}P$ NMR spectrum at *ca.* −70 ppm ($\Delta\delta \approx 30$ ppm with respect to the free PTA ligand). Additionally, in the $^{1}H$ NMR spectra signals corresponding to the methylene protons of PTA ($PCH_2N$ as a singlet at *ca.* 4 ppm and $NCH_2N$ as a multiplet at 4.3–4.5 ppm) are observed. In the aromatic region, two signals are detected for

the protons of the 4-nitrophenyl or 4-trifluoromethyl fragments. Consistently, in the $^{13}C$ NMR spectra, the methylene carbons $PCH_2N$ and $NCH_2N$ resonate as doublets at 52 and 73 ppm, respectively, along with all carbons of the aryl fragment.

Similar considerations can be applied to the dicationic complex **7b**. Particularly diagnostic is the $^{31}P$ NMR spectrum, which present a singlet at −50 ppm, in addition to the septet at −144 ppm of the hexafluorophosphate anion.

Finally, in the case of complexes **7a** and **8a**, the proposed structures were corroborated by XRD analyses (Fig. 2). In this respect, suitable crystals were obtained by slow evaporation of diethylether in a dichloromethane solution of the palladium complex.

Scheme 2D also illustrates our attempts to coordinate a PTA-based ligand to the [PdCl($\eta^3$-allyl)] fragment. Pd(II)-allyl complexes usually exhibit high cytotoxicity against a broad spectrum of cancer cell lines. However, only a subset of these complexes shows good selectivity towards cancer cells.[40,46] Many of these contain a Pd(II)-allyl fragment, one *N*-heterocyclic carbene (NHC), and one PTA ligand. These complexes, with the general formula [Pd(NHC)(PTA)($\eta^3$-allyl)]X (X = $BF_4$, $ClO_4$, OTf), induce cancer cell death through an apoptotic mechanism involving early mitochondrial damage. Moreover, recent studies have demonstrated that such organopalladium derivatives significantly inhibit key proteins involved in cellular redox balance, such as thioredoxin reductase (TrxR).[59,60]

The crucial role of PTA in ensuring good selectivity for the Pd(II)-allyl complexes, prompted us to explore the simple reaction between PTA and the commercially available dimeric precursor [PdCl($\eta^3$-allyl)]$_2$ (compound **9** in Scheme 2D), aiming to synthesize the neutral complex [PdCl(PTA)($\eta^3$-allyl)] (**10a**). This reaction represents the cleavage of the palladium dimeric precursor and the simultaneous coordination of the external ligand.

To our surprise, despite numerous attempts, we constantly obtained a mixture of products that were difficult to identify, whereas the same reaction with classical tertiary phosphines (*e.g.*, $PPh_3$) yielded clean products. Evidently, compound **10a** is either not stable, or parasitic reactions are preventing its formation.

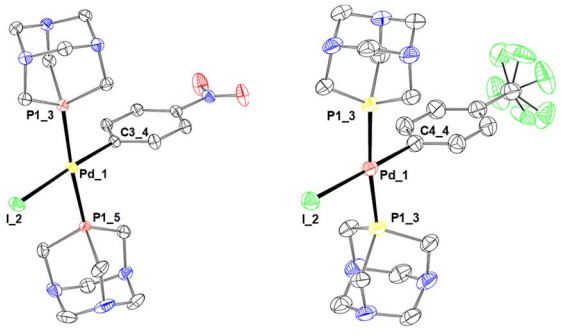


Fig. 2 X-ray molecular structures of **7a** (left) and **8a** (right) are presented, showing thermal displacement ellipsoids at the 50% probability level with hydrogen atoms and solvent molecules omitted for clarity.

However, when the cationic derivative [Me-PTA]$PF_6$ (**b**) was chosen as ligand in the same reaction, the target complex **10b** was obtained without further purification. We therefore hypothesize that the charge of the complex is essential for stabilizing this class of organopalladium derivatives.

The $^{31}P$ NMR spectrum of complex **10b** shows a singlet at *ca.* −39 ppm ($\Delta\delta \approx 48$ ppm with respect to the free PTA ligand), as well as the septet of the $PF_6^-$ counterion at −144 ppm. In the $^1H$ NMR spectrum, it is possible to observe the signals of the methyl protons of the ligand (2.2 ppm) and those of the methylene protons $NCH_2N$ and $NCH_2P$ (multiplets at 4–5 ppm). Regarding the allyl moiety, the multiplet at *ca.* 5.6 ppm is assigned to the central allyl proton, whereas the multiplets for the *anti*-allyl protons are observed at 3.2–3.6 ppm, and those of the *syn*-allyl protons are detected at 4.3–4.6 ppm.

### Synthesis of Pd(II)-imidoyl and Pd(0)-alkene complexes

The last two categories of organopalladium compounds that we considered are Pd(II)-imidoyl and Pd(0)-alkene complexes. Recently, several bisPTA derivatives of these compound classes have been synthesized, including complexes **12a** and **14a** as illustrated in Scheme 2E and F.[47,61] *In vitro* studies have shown that the Pd(II)-imidoyl complex **12a** exhibits moderate cytotoxicity towards ovarian cancer cells ($IC_{50}$ = 28–41 μM),[47] whereas the Pd(0)-alkene complex **14a** displays significant cytotoxicity ($IC_{50}$ = 0.7 μM) against the same cancer cell lines (A2780 and A2780*cis*).[61] Both compounds induce cell death *via* an apoptotic pathway, although a detailed study on the primary biotarget has not yet been carried out.

Following a procedure similar to that used for the synthesis of neutral complexes **12a** and **14a**, their dicationic congeners **12b** and **14b** were obtained. Specifically, a direct reaction was performed between palladium precursors **11** and **13** and two equivalents of [Me-PTA]$PF_6$ (**b**) in acetonitrile at room temperature.

The $^{31}P$ NMR spectra of complexes **12b** and **14b** showed a singlet at −49 and −43 ppm, respectively ($\Delta\delta \approx 40$ ppm with respect to the free [Me-PTA]$PF_6$ ligand), as well as the septet of the $PF_6^-$ counterion at −144 ppm.

In the $^1H$ NMR spectrum of complex **12b**, the methyl protons of the imidoyl fragment and the PTA-based ligands are observed at 2.1–2.8 ppm, the methylene protons $NCH_2N$ and $NCH_2P$ appear as multiplets between 4 and 5 ppm, and the aromatic protons are detectable at 7–7.5 ppm.

For what concerns the $^1H$ NMR spectrum of complex **14b**, in addition to the signals of aromatic protons and those of the PTA-based ligands, the ones of the two olefinic protons are particularly noteworthy, resonating as multiplets between 3.9 and 4.3 ppm. In fact, these protons resonate at 7–8 ppm in the case of free (*E*)-1,2-ditosylethene, thus confirming the coordination of both the phosphine ligand and the alkene to the palladium metal center. The choice of this olefin is due to its ability to form a very robust bond with palladium, attributed to strong back-donation. The high stability of Pd(0)–(*E*)-ditosylethene derivatives is expected to reduce or prevent the hydrolysis of the complex before it reaches the biotarget.

### Antiproliferative activity on human cancer and normal cell lines

With the aim of studying the potential antitumor activity of the organopalladium complexes bearing PTA-based ligands, a panel of four different human tumor cell lines (ovarian cancer A2780, with its cisplatin resistant clone A2780*cis*, triple-negative breast cancer MDA-MB231 and U87 glioblastoma) and MRC-5 non-cancerous cells were treated for 96 h with the synthesized compounds and cisplatin.

Preliminarily, we have monitored the stability of the organopalladium complexes in a solution containing *ca.* 2 mg of Pd complex dissolved in a DMSO/$H_2O$ mixture (0.15 mL: 250 mL) with 1.46 g of NaCl (0.1 M). After 24 h no significant changes of the spectra are detectable, indicating that the complexes retain their structural integrity. We have additionally monitored the stability in a 1 : 2 culture medium/DMSO-$d_6$ solution by $^{31}P$ NMR (Fig. S51–S61 in ESI†). The complexes were stable even under these conditions.

The antiproliferative activity results for the tested compounds are reported in Table 1 in terms of half inhibitory concentrations ($IC_{50}$) values.

Analyzing the data obtained from A2780 cisplatin-sensitive ovarian cancer cells, it is evident that all the compounds synthesized in this study exhibit cytotoxicity comparable to or greater than cisplatin, with some showing up to an order of magnitude higher activity. Notably, among compounds with the same phosphine ligand, the Pd(II)-butadienyl complexes (**4a–e**) are generally more active than their Pd(II)-vinyl counterparts (**3a–e**). Within the Pd(II)-butadienyl series, the phosphine ligand exerts a significant influence; complexes containing PTA or its cationic derivatives (**d–e**) demonstrate higher activity compared to those with ligands **b** and **c**. Similarly, among the Pd(II)-aryl complexes, those containing PTA (**7a** and **8a**) are more active than the dicationic derivative **7b**. Nevertheless, **7b** still exhibits good cytotoxicity, comparable to that of cisplatin.

For Pd(II)-imidoyl and Pd(0)-alkene complexes (**12a–b** and **14a–b**), the dicationic compounds (**12b** and **14b**) display cytotoxicity comparable to or even greater than their neutral congeners.

Even more interesting are the results obtained with cisplatin-resistant ovarian cancer cells (A2780*cis*). All the compounds, except for **12a**, show cytotoxicity that is one or two orders of magnitude higher than that of cisplatin. As observed on A2780 cancer cells, the Pd(II)-butadienyl (**4a–e**), Pd(II)-aryl (**7a–b** and **8a**), and Pd(0)-alkene (**14a–b**) complexes are more active than their Pd(II)-vinyl (**3a–e**), Pd(II)-allyl (**10b**), and Pd(II)-imidoyl (**12a–b**) congeners.

When exploring a completely different cancer model, such as triple-negative breast cancer cells (MDA-MB-231), the results highlight the high efficacy of complexes containing unfunctionalized PTA (**3a**, **4a**, **7a**, **8a**), regardless of the type of organopalladium fragment. The cationic complexes (**3b–e**, **4b–c**, **4e**, **7b**, **10b**, and **14b**) also demonstrate good cytotoxicity, comparable to that of cisplatin, while derivatives **4d** and **12b** are scarcely active.

Although the ovarian cancer and triple-negative breast cancer cells revealed good to excellent cytotoxicity for the complexes investigated in this study, this trend does not extend to glioblastoma (U87) cells. The $IC_{50}$ values presented in Table 1 show that most compounds are poorly active or inactive against this tumor type. Exceptions include complexes **4e**, **10b**, and **14b**,

Table 1 Antiproliferative activity on A2780, A2780*cis*, MDA-MB-231, U87 and MRC-5 cell lines[a]

| | $IC_{50}$ (μM) | | | | |
|---|---|---|---|---|---|
| Compound | A2780 | A2780*cis* | MDA-MB-231 | U87 | MRC-5 |
| Cisplatin | 2.7 ± 0.3 | 45 ± 5 | 10 ± 1 | 10.4 ± 0.4 | 4 ± 1 |
| **3a** (ref. 39) | 0.17 ± 0.04 | 2.2 ± 0.3 | 0.3 ± 0.1 | — | >100 |
| **3b** | 3.4 ± 0.4 | 0.56 ± 0.08 | 14 ± 2 | 80 ± 10 | >100 |
| **3c** | 2.7 ± 0.2 | 2.1 ± 0.2 | 15 ± 2 | >100 | >100 |
| **3d** | 1.3 ± 0.3 | 1.3 ± 0.2 | 9 ± 1 | 60 ± 10 | >100 |
| **3e** | 2.9 ± 0.1 | 2.2 ± 0.1 | 14 ± 1 | 80 ± 10 | >100 |
| **4a** (ref. 39) | 0.08 ± 0.04 | 0.6 ± 0.4 | 0.10 ± 0.01 | — | >100 |
| **4b** | 3.3 ± 0.5 | 0.44 ± 0.08 | 9 ± 1 | 70 ± 10 | >100 |
| **4c** | 3.0 ± 0.6 | 0.90 ± 0.08 | 9 ± 2 | 80 ± 10 | >100 |
| **4d** | 0.55 ± 0.09 | 0.33 ± 0.05 | 80 ± 10 | 90 ± 20 | 90 ± 10 |
| **4e** | 0.29 ± 0.02 | 0.43 ± 0.07 | 10 ± 1 | 15 ± 6 | 70 ± 10 |
| **7a** | 0.31 ± 0.02 | 0.29 ± 0.07 | 0.50 ± 0.04 | 80 ± 20 | >100 |
| **7b** | 3.1 ± 0.3 | 0.18 ± 0.02 | 6.7 ± 0.9 | 90 ± 10 | >100 |
| **8a** | 0.43 ± 0.09 | 0.31 ± 0.03 | 0.6 ± 0.2 | 30 ± 10 | >100 |
| **10b** | 3.7 ± 0.2 | 1.9 ± 0.5 | 15 ± 2 | 15 ± 5 | >100 |
| **12a** (ref. 47) | 30 ± 10 | 41 ± 5 | — | — | — |
| **12b** | 4.7 ± 0.4 | 3.5 ± 0.2 | 80 ± 10 | 60 ± 10 | 80 ± 10 |
| **14a** (ref. 61) | 0.7 ± 0.3 | 0.7 ± 0.1 | — | — | — |
| **14b** | 0.61 ± 0.04 | 0.35 ± 0.05 | 3.1 ± 0.3 | 3.0 ± 0.2 | 80 ± 10 |

[a] Data after 96 h of incubation. Stock solutions in DMSO for all complexes; stock solutions in $H_2O$ for cisplatin. A2780 (cisplatin-sensitive ovarian cancer cells), A2780*cis* (cisplatin-resistant ovarian cancer cells), MDA-MB-231 (triple-negative breast cancer), U87 (glioblastoma) and MRC-5 (normal lung fibroblasts).

which exhibit cytotoxicity comparable to or exceeding that of cisplatin.

Given that most of the analysed compounds show selectivity toward ovarian and breast cancer cells, we also investigated their cytotoxicity against non-cancerous cells (MRC-5). To our delight and surprise, nearly all compounds are poorly active or inactive against normal cells, highlighting their pronounced *in vitro* selectivity. In contrast, cisplatin exhibits comparable cytotoxicity towards both cancerous and non-cancerous cells.

### Molecular docking studies

One of the most promising complexes among those tested, namely **8a**, belongs to the palladium–aryl family. These compounds have recently been studied from a biological perspective and exhibit DNA as their primary target.[49]

To better understand the binding interactions between DNA and the fully optimized structure of **8a**, we carried out molecular docking simulations.

The palladium complex binds in the minor groove of the DNA and exhibits hydrogen bonds (H-bonds), carbon–hydrogen (C–H) bonds, and Pd···O intermolecular interactions (Fig. 3). These interactions are crucial for stabilizing the ligand–receptor complex both geometrically and energetically. In fact, the predicted binding free energy ($\Delta G$) of −6.9 kcal mol$^{-1}$ suggests that **8a** has a higher affinity for DNA than another palladium complex ([PdI(Ph)(dppe)]) from our previous study,[49] which is nicely consistent with its superior cytotoxicity. The H-bond forms between a deoxyguanosine residue (dG22) of DNA and the nitrogen atom of **8a**, while the two C–H bond interactions involve the trifluoromethyl group of **8a** and the C–H moieties of the DNA sugar backbone.

Additionally, the Lewis acid–base interaction — specifically, the interaction between the palladium metal and the oxygen atom of the sugar in the dC23 residue (Pd···O) — plays an important role in the binding pose of the molecule, orienting the Pd–I moiety (polar region of the ligand) toward the solvent-accessible area (water) and outside the DNA hydrophobic groove.

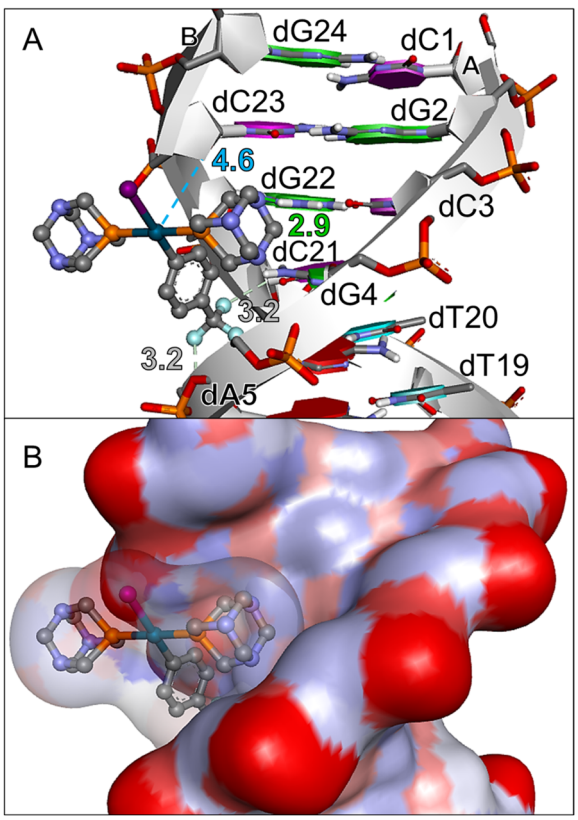


Fig. 3 DNA interactions with complex **8a**. (A) Binding pose and interactions between DNA and **8a**. (B) Surface model coloured by atomic charges. The DNA is represented by strands and rings, with deoxyadenosine (dA), deoxythymidine (dT), deoxycytidine (dC), and deoxyguanosine (dG) residues shown in red, blue, pink, and green, respectively. Molecular interactions, including hydrogen bonds, carbon-hydrogen bonds, and palladium···oxygen (Pd···O) contacts, are depicted by green, grey, and cyan dashed lines, respectively, with distances in Å.

## Conclusions

In this study, we report the synthesis of 15 novel organopalladium complexes featuring PTA-based ligands. Most of the newly synthesized compounds incorporate PTA cationic derivatives as ancillary ligands, which were preliminarily prepared as hexafluorophosphate salts to prevent halide exchange reactions at the metal center.

A variety of organopalladium fragments were explored, including Pd(II)-vinyl, Pd(II)-butadienyl, Pd(II)-allyl, Pd(II)-imidoyl, Pd(II)-aryl, and Pd(0)-alkene, which have recently demonstrated promising antiproliferative activity against various cancer cell lines. Reactions between PTA-based ligands and the different palladium precursors investigated proceed within 30 min at room temperature under aerobic conditions, utilizing non-anhydrous acetonitrile or dichloromethane as solvents.

Interestingly, in the case of the Pd(II)-allyl fragment, the PTA derivative proved unstable and could not be isolated. Conversely, the cationic derivative incorporating MePTA$^+$ as a ligand was isolable and sufficiently stable to allow biological testing.

All newly synthesized compounds were fully characterized by $^1$H, $^{13}$C, and $^{31}$P NMR spectroscopy and elemental analyses. For complexes **7a** and **8a**, their structures were further confirmed by single-crystal X-ray diffraction analysis.

To evaluate the antitumor potential of organopalladium complexes with PTA-based ligands, we tested them on four human tumor cell lines—A2780 ovarian cancer, its cisplatin-resistant clone A2780*cis*, MDA-MB-231 triple-negative breast cancer, and U87 glioblastoma—as well as on MRC-5 non-cancerous cells. The $IC_{50}$ values highlight the remarkable cytotoxicity (in the micro- or submicro-molar range) of all tested organopalladium compounds against ovarian cancer and triple-negative breast cancer cells. This cytotoxicity is comparable to or significantly higher than that of cisplatin (reference drug) with some compounds showing activity up to two orders of magnitude greater. Among the tested categories, complexes featuring Pd(II)-butadienyl, Pd(II)-aryl, and Pd(0)-alkene

fragments proved more active than those containing Pd(II)-vinyl, Pd(II)-allyl, and Pd(II)-imidoyl fragments.

For a given organopalladium fragment, complexes containing PTA as a ligand generally displayed higher activity compared to those with cationic PTA ligands. Curiously, nearly all tested compounds exhibited minimal or no activity ($IC_{50}$ > 100 μM) against non-cancerous MRC-5 human lung fibroblasts, proving high *in vitro* selectivity for cancer cells over normal ones. In contrast, as reported in previous studies, cisplatin exhibited comparable cytotoxicity towards both cancerous and normal cells.

A downside of this work deals with the results obtained on the glioblastoma cell line (U87), where only complexes **4e**, **10b**, and above all **14b** displayed an encouraging cytotoxicity ($IC_{50}$ = 3–15 μM).

Overall, we consider complexes **7a**, **8a**, and **14b** to be the most promising, alongside some previously investigated compounds (**3a** and **4a**). Molecular docking simulations between DNA and **8a** revealed that the interaction with the minor groove is stabilized by hydrogen bonds, C–H interactions, and a Pd···O Lewis acid–base interaction, contributing to a favourable binding free energy of −6.9 kcal $mol^{-1}$. These findings are consistent with the higher cytotoxicity of **8a** compared to previously studied Pd(II)-aryl complexes, highlighting its potential as a biologically active compound.

Complex **14b** is also particularly interesting as it is the only one that presents palladium in the zerovalent state, which is decidedly less explored in medicinal chemistry compared to Pd(II) complexes, and it is the only one active on all the investigated tumor cell lines, including glioblastoma.

Based on these promising results, further *in vitro* and *in vivo* experiments, as well as detailed mechanistic studies, are currently underway in our laboratories.

# Experimental

Dichloromethane and acetonitrile were dried using 4 Å molecular sieves. All other solvents and chemicals were commercial grade products and used as purchased. In particular, 1,3,5-triaza-7-phosphaadamantane (PTA), methyl iodide, dichloromethane, acetonitrile, acetone, diethyl ether, pentane, potassium hexafluorophosphate, 2-bromoethyl acetate, 4-(bromomethyl)benzoic acid, 5-(chloromethyl)-2-hydroxybenzaldehyde were purchased from Sigma-Aldrich (Merck). The same supplier provided us with the cell lines used in the biological part.

Palladium precursors **1–2**,[62] **5–6**,[63,64] **11**,[47] **13** (ref. 61) were synthesized according to published protocols.

1D-NMR and 2D-NMR spectra were recorded on Bruker 300 or 400 Advance spectrometers. Chemical shifts values (ppm) are given relative to TMS ($^1$H and $^{13}$C), $H_3PO_4$ ($^{31}$P) and $CCl_3F$ ($^{19}$F). Elemental analyses were carried out using an Elemental CHN "CUBO Micro Vario" analyzer.

### Synthesis of PTA-based ligands

**Synthesis of ligand b.** In a 100 mL round bottom flask, 0.3501 g (2.227 mmol) of 1,3,5-triaza-7-phosphaadamantane (PTA) and 0.3280 g (2.311 mmol) of methyl iodide were dissolved in 30 mL of acetone. The mixture was maintained under reflux conditions for 1 h. Afterwards, the mixture was filtered on a sintered glass filter, affording a white solid, which was washed with cold acetone and diethyl ether, and dried under vacuum.

The iodide counterion was replaced by hexafluorophosphate by dissolving the white solid in 15 mL of distilled water in the presence of 0.5330 g (2.895 mmol) of $KPF_6$. The solution was kept at room temperature for 30 min and then filtered in a sintered glass filter. The final product was dried under vacuum and obtained as white solid (0.4940 g, yield = 70%).

$^1$H NMR (300 MHz, DMSO-$d_6$, 298 K, ppm) $\delta$: 2.58 (s, 3H, $NCH_3$), 3.71–4.94 (m, 12H, $NCH_2N$, $NCH_2P$).

$^{31}$P{$^1$H}-NMR (121 MHz, DMSO-$d_6$, 298 K, ppm) $\delta$: −87.0, −144.2 (sept, $J$ = 701 Hz, $PF_6^-$).

**Synthesis of ligand c.** In a 100 mL round bottom flask, 0.2714 g (1.727 mmol) of 1,3,5-triaza-7-phosphaadamantane (PTA) and 1.368 g (8.242 mmol) of 2-bromoethyl acetate were dissolved in 30 mL of acetone. The mixture was maintained under reflux conditions for 3 h. Afterwards, the mixture was filtered on a sintered glass filter, affording a white solid, which was washed with cold acetone and diethyl ether, and dried under vacuum.

The bromide counterion was replaced by hexafluorophosphate by dissolving the white solid in 20 mL of distilled water in the presence of 0.4133 g (2.895 mmol) of $KPF_6$. The solution was kept at room temperature for 30 min and then filtered in a sintered glass filter. The final product was dried under vacuum and obtained as white solid (0.4102 g, yield = 61%).

$^1$H NMR (300 MHz, DMSO-$d_6$, 298 K, ppm) $\delta$: 2.08 (s, 3H, $CH_3$), 3.76–4.60 (m, 12H, $NCH_2N$, $NCH_2P$), 4.84–5.09 (m, 4H, $NCH_2CH_2O$).

$^{31}$P{$^1$H}-NMR (121 MHz, DMSO-$d_6$, 298 K, ppm) $\delta$: −85.3, −144.2 (sept, $J$ = 711.3 Hz, $PF_6^-$).

**Synthesis of ligand d.** In a 100 mL round bottom flask, 0.1571 g (1.000 mmol) of 1,3,5-triaza-7-phosphaadamantane (PTA) and 0.2583 g (1.2011 mmol) of 4-(bromomethyl)benzoic acid were dissolved in 20 mL of acetone. The mixture was maintained for 2 h at room temperature. Afterwards, the mixture was filtered on a sintered glass filter, affording a white solid, which was washed with cold acetone and diethyl ether, and dried under vacuum.

The bromide counterion was replaced by hexafluorophosphate by dissolving the white solid in 15 mL of distilled water in the presence of 0.2304 g (1.252 mmol) of $KPF_6$. The solution was kept at room temperature for 30 min and then filtered in a sintered glass filter. The final product was dried under vacuum and obtained as a white solid (0.3586 g, yield = 82%).

$^1$H NMR (300 MHz, DMSO-$d_6$, 298 K, ppm) $\delta$: 3.92–3.77 (m, 4H, $NCH_2P$), 4.14 (s, 2H, $NCH_2Ph$), 4.24 (d, $J$ = 5.8 Hz, 2H, $NCH_2P$), 4.55 and 4.35 (AB system, $J_{AB}$ = 12.0 Hz, 2H, $NCH_2N$), 5.03 and 4.87 (AB system, $J_{AB}$ = 12.0 Hz, 4H, $NCH_2N$), 8.07 and 7.63 (m, 4H, Ar–H).

$^{31}$P{$^1$H}-NMR (121 MHz, DMSO-$d_6$, 298 K, ppm) $\delta$: −83.4, −144.1 (sept, $J$ = 711.2 Hz, $PF_6^-$).

**Synthesis of ligand e.** In a 100 mL round bottom flask, 0.1571 g (1.000 mmol) of 1,3,5-triaza-7-phosphaadamantane (PTA) and 0.1970 g (1.155 mmol) of 5-(chloromethyl)-2-hydroxybenzaldehyde were dissolved in 20 mL of acetone. The mixture was maintained under reflux conditions for 2 h. Afterwards, the mixture was filtered on a sintered glass filter, affording a white solid, which was washed with cold acetone and diethyl ether, and dried under vacuum.

The bromide counterion was replaced by hexafluorophosphate by dissolving the white solid in 15 mL of distilled water in the presence of 0.2306 g (1.252 mmol) of $KPF_6$. The solution was kept at room temperature for 30 min and then filtered in a sintered glass filter. The final product was dried under vacuum and obtained as a white solid (0.3458 g, yield = 79%).

$^1$H NMR (300 MHz, $CH_3CN$-$d_3$, 298 K, ppm) $\delta$: 3.73–3.96 (m, 4H, $NCH_2P$), 4.00 (s, 2H, $NCH_2Ph$), 4.11–4.14 (m, 2H, $NCH_2P$), 4.38–4.58 (m, 2H, $NCH_2N$), 4.77–4.89 (m, 4H, $NCH_2N$), 7.13–7.83 (3H, Ar–H), 10.32 (d, $J$ = 0.6 Hz, 1H, CHO), 11.12 (s, 1H, OH).

$^{31}P\{^1H\}$-NMR (121 MHz, DMSO-$d_6$, 298 K, ppm) $\delta$: −82.6, −144.6 (sept, $J$ = 711.2 Hz, $PF_6^-$).

### Synthesis of neutral organopalladium complexes bearing PTA

**Synthesis of complex 7a.** To 0.0606 g (0.128 mmol) of [PdI(tmeda)(*p*-$NO_2$-Ph)] (**5**) dissolved in 5 mL of anhydrous $CH_2Cl_2$, a solution of 0.0408 g (0.260 mmol) of PTA in 5 mL of anhydrous $CH_2Cl_2$ was added under inert atmosphere (Ar). The resulting yellow solution was stirred for 30 min at room temperature. The solution was then concentrated under vacuum and the title complex was precipitated by addition of diethyl ether and pentane, was filtered through a sintered glass filter, and dried under vacuum. 0.0799 g (yield 93%) of complex **7a** was obtained as a yellow powder.

$^1$H NMR (300 MHz, $CDCl_3$, 298 K, ppm) $\delta$: 4.00 (s, 12H, $PCH_2N$), 4.32–4.45 (m, 12H, $NCH_2N$), 7.40 (d, 2H, $J$ = 8.2 Hz, Ar–H), 8.02 (d, 2H, $J$ = 8.2 Hz, Ar–H).

$^{13}C\{^1H\}$-NMR (75 MHz, $CDCl_3$, 298 K, ppm) $\delta$: 52.1 ($CH_2$, t, $J_{C-P}$ = 7.4 Hz, $PCH_2N$), 73.2 ($CH_2$, t, $J_{C-P}$ = 3.6 Hz, $NCH_2N$), 122.3 (CH, Ar–CH), 136.0 (CH, t, $J_{C-P}$ = 4.8 Hz, Ar–CH), 145.8 (C, *p*-Ar–C), 163.8 (C, t, $J_{C-P}$ = 7.5 Hz, *i*-Ar–C).

$^{31}P\{^1H\}$-NMR (121 MHz, $CDCl_3$, 298 K, ppm) $\delta$: −69.5.

Elemental analysis calcd (%) for $C_{18}H_{28}IN_7O_2P_2Pd$: C, 32.28, H, 4.21, N, 14.64; found: C, 32.57, H, 4.04, N, 14.73.

**Synthesis of complex 8a.** Complex **8a** was obtained in the same manner as complex **7a** by employing 0.0559 g (0.113 mmol) of [PdI(tmeda)(*p*-$CF_3$-Ph)] (**6**) dissolved in 5 mL of anhydrous $CH_2Cl_2$ and 0.0359 g (0.228 mmol) of PTA in 5 mL of anhydrous $CH_2Cl_2$. Complex **8a** was precipitated by addition of diethyl ether. 0.0733 g (yield 94%) of complex **8a** was obtained as a yellow solid.

$^1$H NMR (300 MHz, $CDCl_3$, 298 K, ppm) $\delta$: 3.99 (s, 12H, $PCH_2N$), 4.33–4.44 (m, 12H, $NCH_2N$), 7.28 (d, 2H, $J$ = 8.1 Hz, Ar–H), 7.40 (d, 2H, $J$ = 7.8 Hz, Ar–H).

$^{13}C\{^1H\}$-NMR (75 MHz, $CDCl_3$, 298 K, ppm) $\delta$: 52.0 ($CH_2$, t, $J_{C-P}$ = 7.4 Hz, $PCH_2N$), 73.2 ($CH_2$, t, $J_{C-P}$ = 3.3 Hz, $NCH_2N$), 124.9 (CH, q, $J_{C-F}$ = 3.7 Hz, Ar–CH), 126.6 (C, q, $J_{C-F}$ = 27.5 Hz, *p*-Ar–C), 135.9 (CH, t, $J_{C-P}$ = 4.8 Hz, Ar–CH), 155.3 (C, t, $J_{C-P}$ = 6.7 Hz, *i*-Ar–C).

$^{31}P\{^1H\}$-NMR (121 MHz, $CDCl_3$, 298 K, ppm) $\delta$: −69.3.

Elemental analysis calcd (%) for $C_{19}H_{28}F_3IN_6P_2Pd$: C, 32.94, H, 4.07, N, 12.13; found: C, 32.70, H, 4.15, N, 12.24.

### Synthesis of cationic and dicationic organopalladium complexes bearing PTA-based ligands

**Synthesis of complex 3b.** To 0.0457 g (0.0888 mmol) of palladium precursor **1** dissolved in 15 mL of anhydrous $CH_3CN$, 0.0564 g (0.1777 mmol) of ligand **b** was added. The resulting colourless solution was stirred for 30 min at room temperature. The solvent was removed under vacuum and the title complex was precipitated from a $CH_2Cl_2$/$Et_2O$ solution, filtered through a sintered glass filter, and dried under vacuum. 0.0705 g (yield 85%) of complex **3b** was obtained as a pale-yellow powder.

$^1$H NMR (300 MHz, $CH_3CN$-$d_3$, 298 K, ppm) $\delta$: 1.96 (s, 3H, $=CCH_3$), 2.76 (s, 6H, $NCH_3$), 3.67 (s, 3H, $OCH_3$), 3.78 (s, 3H, $OCH_3$), 4.07–4.95 (m, 24H, $NCH_2N$, $NCH_2P$).

$^{13}C\{^1H\}$-NMR (75 MHz, $CH_3CN$-$d_3$, 298 K, ppm) $\delta$: 171.6, 162.9, 129.1, 80.9, 69.1, 54.7, 52.1, 51.9, 51.5, 51.4, 49.3, 46.4, 46.3, 40.4, 22.1.

$^{31}P\{^1H\}$-NMR (121 MHz, $CH_3CN$-$d_3$, 298 K, ppm) $\delta$: −43.6, −144.6 (sept, $J$ = 701 Hz, $PF_6^-$).

Elemental analysis calcd (%) for $C_{21}H_{39}ClF_{12}N_6O_4P_4Pd$: C, 27.02, H, 4.21, N, 9.00; found: C, 26.85, H, 4.29, N, 9.11.

**Synthesis of complex 3c.** Complex **3c** was obtained in the same manner as complex **3b** by employing 0.0522 g (0.1015 mmol) of precursor **1** dissolved in 15 mL of anhydrous $CH_3CN$ and 0.0791 g (0.203 mmol) of ligand **c**. 0.0719 g (yield 66%) of complex **3c** was obtained as a white solid.

$^1$H NMR (300 MHz, $CH_3CN$-$d_3$, 298 K, ppm) $\delta$: 1.96 (s, 3H, $=CCH_3$), 2.12 (s, 6H, O–$COCH_3$), 3.26–3.38 (m, 4H, $N^+C\underline{H_2}CH_2O$), 3.67 (s, 3H, $OCH_3$) 3.78 (s, 3H, $OCH_3$), 4.11–5.12 (m, 24H, $NCH_2N$, $NCH_2P$), 4.37–4.42 (m, 4H, $N^+CH_2C\underline{H_2}O$).

$^{13}C\{^1H\}$-NMR (75 MHz, $CH_3CN$-$d_3$, 298 K, ppm) $\delta$: 170.3, 169.8, 129.0, 82.6, 80.6, 73.2, 59.8, 51.4, 49.2, 40.4, 19.9.

$^{31}P\{^1H\}$-NMR (121 MHz, $CH_3CN$-$d_3$, 298 K, ppm) $\delta$: −42.2, −144.6 (sept, $J$ = 718 Hz, $PF_6^-$).

Elemental analysis calcd (%) for $C_{27}H_{47}ClF_{12}N_6O_8P_4Pd$: C, 30.10, H, 4.40, N, 7.80; found: C, 30.46, H, 4.25, N, 7.71.

**Synthesis of complex 3d.** Complex **3d** was obtained in the same manner as complex **3b** by employing 0.0527 g (0.102 mmol) of precursor **1** dissolved in 15 mL of anhydrous $CH_3CN$ and 0.0896 g (0.205 mmol) of ligand **d.** 0.0899 g (yield 75%) of complex **3d** was obtained as a white solid.

$^1$H NMR (300 MHz, $CH_3CN$-$d_3$, 298 K, ppm) $\delta$: 1.96 (s, 3H, $=CCH_3$), 2.05 (s, 4H, $CH_2$), 3.60 (s, 3H, $OCH_3$), 3.73 (s, 3H, $OCH_3$), 3.89–4.90 (m, 24H, $NCH_2N$, $NCH_2P$), 7.16 (d, 2H, $J$ = 8.53 Hz, Ar–H) 7.59 (d, 2H, $J$ = 8.41 Hz, Ar–H), 7.78 (s, 2H, Ar–H), 10.02 (s, 2H, CHO), 11.12 (s, 2H, OH).

$^{13}C\{^1H\}$-NMR (75 MHz, $CH_3CN$-$d_3$, 298 K, ppm) $\delta$: 192.4, 172.0, 166.2, 133.2, 130.7, 130.4, 130.2, 129.4, 129.1, 127.0, 82.7, 80.9, 51.1, 49.3, 46.3, 40.2, 18.2.

$^{31}P\{^1H\}$-NMR (121 MHz, $CH_3CN$-$d_3$, 298 K, ppm) $\delta$: −40.3, −144.5 (sept, $J$ = 693 Hz, $PF_6^-$).

Elemental analysis calcd (%) for $C_{35}H_{47}ClF_{12}N_6O_8P_4Pd$: C, 35.82, H, 4.04, N, 7.16; found: C, 36.07, H, 3.91, N, 7.03.

**Synthesis of complex 3e.** Complex **3e** was obtained in the same manner as complex **3b** by employing 0.0526 g (0.102 mmol) of precursor **1** dissolved in 15 mL of anhydrous $CH_3CN$ and 0.0897 g (0.205 mmol) of ligand **e**. 0.117 g (yield 93%) of complex **3e** was obtained as a white solid.

$^1$H NMR (300 MHz, $CH_3CN$-$d_3$, 298 K, ppm) $\delta$: 1.97 (s, 3H, $=CCH_3$), 2.02 (s, 4H, $CH_2$), 2.23 (bs, 1H, COOH), 3.59 (s, 3H, $OCH_3$), 3.75 (s, 3H, $OCH_3$), 3.89–5.05 (m, 24H, $NCH_2N$, $NCH_2P$), 7.14–7.41 (m, Ar–H), 7.56 (d, $J$ = 7.60 Hz, Ar–H), 8.15 (d, $J$ = 7.83 Hz, Ar–H).

$^{13}$C{$^1$H}-NMR (75 MHz, $CH_3CN$-$d_3$, 298 K, ppm) $\delta$: 197.4, 190.3, 165.7, 162.8, 140.7, 138.7, 136.8, 136.7, 135.1, 132.5, 129.5, 121.2, 121.0, 120.7, 82.7, 80.9, 79.4, 79.3, 69.3, 64.6, 51.6, 51.5, 50.7, 49.3, 46.3, 40.3, 22.1.

$^{31}$P{$^1$H}-NMR (121 MHz, $CH_3CN$-$d_3$, 298 K, ppm) $\delta$: −40.1, −144.6 (sept, $J$ = 705 Hz, $PF_6^-$).

Elemental analysis calcd (%) for $C_{35}H_{47}ClF_{12}N_6O_8P_4Pd$: C, 35.82, H, 4.04, N, 7.16; found: C, 35.60, H, 4.12, N, 7.21.

**Synthesis of complex 4b.** To 0.0471 g (0.0717 mmol) of palladium precursor **2** dissolved in 10 mL of anhydrous $CH_3CN$, 0.0455 g (0.144 mmol) of ligand **b** was added. The resulting colourless solution was stirred for 30 min at room temperature. The solvent was removed under vacuum and the title complex was precipitated from a $CH_2Cl_2$/$Et_2O$ solution, filtered through a sintered glass filter, and dried under vacuum. 0.0750 g (yield 97%) of complex **4b** was obtained as a white powder.

$^1$H NMR (300 MHz, $CH_3CN$-$d_3$, 298 K, ppm) $\delta$: 1.8–2.0 (m, 3H, $=CCH_3$), 2.8 (s, 6H, $NCH_3$), 3.72 (s, 3H, $OCH_3$), 3.81 (s, 3H, $OCH_3$), 3.82 (s, 3H, $OCH_3$), 3.85 (s, 3H, $OCH_3$), 4.11–4.99 (m, 24H, $NCH_2N$, $NCH_2P$).

$^{13}$C{$^1$H}-NMR (75 MHz, $CH_3CN$-$d_3$, 298 K, ppm) $\delta$: 169.0, 161.7, 138.2, 134.2, 81.1, 69.2, 54.8, 53.2, 52.7, 52.2, 49.3, 46.4, 40.4, 17.5.

$^{31}$P{$^1$H}-NMR (121 MHz, $CH_3CN$-$d_3$, 298 K, ppm) $\delta$: −42.2, −144.6 (sept, $J$ = 706.5 Hz, $PF_6^-$).

Elemental analysis calcd (%) for $C_{27}H_{45}ClF_{12}N_6O_8P_4Pd$: C, 30.15, H, 4.22, N, 7.81; found: C, 30.40, H, 4.08, N, 7.71.

**Synthesis of complex 4c.** Complex **4c** was obtained in the same manner as complex **4b** by employing 0.0502 g (0.0764 mmol) of precursor **2** dissolved in 11 mL of anhydrous $CH_3CN$ and 0.0597 g (0.1534 mmol) of ligand **c**. 0.0502 g (yield 54%) of complex **4c** was obtained as a white solid.

$^1$H NMR (300 MHz, $CH_3CN$-$d_3$, 298 K, ppm) $\delta$: 1.8–2.0 (s, 3H, $=CCH_3$), 2.13 (s, 6H, $OCOCH_3$), 3.34 (s, 4H, $NCH_2N$), 3.72 (s, 3H, $OCH_3$), 3.74 (s, 3H, $OCH_3$), 3.81 (s, 3H, $OCH_3$), 3.85 (s, 3H, $OCH_3$), 4.08–4.35 (m, 8H, $CH_2CH_2$), 4.37–4.61 (m, 12H, $NCH_2P$), 4,99 (m, 8H, $NCH_2N$).

$^{13}$C{$^1$H}-NMR (75 MHz, $CH_3CN$-$d_3$, 298 K, ppm) $\delta$: 171.1, 171.0, 162.4, 139.1, 83.7, 83.6, 81.8, 74.0, 60.4, 53.5, 53.1, 49.9, 41.1, 20.7, 18.3.

$^{31}$P{$^1$H}-NMR (121 MHz, $CH_3CN$-$d_3$, 298 K, ppm) $\delta$: −40.1, −144.6 (sept, $J$ = 706.3 Hz, $PF_6^-$).

Elemental analysis calcd (%) for $C_{33}H_{53}ClF_{12}N_6O_{12}P_4Pd$: C, 32.50, H, 4.38, N, 6.89; found: C, 32.14, H, 4.50, N, 6.98.

**Synthesis of complex 4d.** Complex **4d** was obtained in the same manner as complex **4b** by employing 0.0680 g (0.1035 mmol) of precursor **2** dissolved in 11 mL of anhydrous $CH_3CN$ and 0.0904 g (0.2068 mmol) of ligand **d**. 0.1314 g (yield 98%) of complex **4d** was obtained as a white solid.

$^1$H NMR (300 MHz, $CH_3CN$-$d_3$, 298 K, ppm) $\delta$: 1.79 (s, 3H, $=CCH_3$), 3.69 (s, 3H, $OCH_3$), 3.72 (s, 3H, $OCH_3$), 3.73 (s, 3H, $OCH_3$), 3.78 (s, 3H, $OCH_3$), 4.15-4-60 (m, 16H, $NCH_2N$, $NCH_2P$), 4.80–5.01 (m, 8H, $NCH_2N$, $NCH_2P$), 4.89 (s, 2H, OH), 7.13–7.19 (d, 2H, $J$ = 8.6 Hz, Ar–H), 7.57–7.65 (dd, 2H, $J$ = 8.6 Hz, $J$ = 2.3 Hz, Ar–H), 7.77–7.82 (d, 2H, $J$ = 2.3 Hz, Ar–H), 10.02 (s, 2H, CHO).

$^{13}$C{$^1$H}-NMR (75 MHz, $CH_3CN$-$d_3$, 298 K, ppm) $\delta$: 192.9, 166.7, 166.5, 138.4, 133.8, 131.3, 131.0, 130.8, 130.0, 129.6, 127.5.

$^{31}$P{$^1$H}-NMR (121 MHz, $CH_3CN$-$d_3$, 298 K, ppm) $\delta$: 38.9, −144.6 (sept, $J$ = 706.6 Hz, $PF_6^-$).

Elemental analysis calcd (%) for $C_{41}H_{53}ClF_{12}N_6O_{12}P_4Pd$: C, 37.43, H, 4.06, N, 6.39; found: C, 37.61, H, 3.98, N, 6.48.

**Synthesis of complex 4e.** Complex **4e** was obtained in the same manner as complex **4b** by employing 0.0677 g (0.1029 mmol) of precursor **2** dissolved in 15 mL of anhydrous $CH_3CN$ and 20 mL of MeOH and 0.0900 g (0.2059 mmol) of ligand **e**. 0.1294 g (yield 97%) of complex **4e** was obtained as a white solid.

$^1$H NMR (300 MHz, $CH_3CN$-$d_3$, 298 K, ppm) $\delta$: 1.77 (s, 3H, $=CCH_3$), 3.65 (s, 3H, $OCH_3$), 3.71 (s, 3H, $OCH_3$), 3.75 (s, 3H, $OCH_3$), 3.77 (s, 3H, $OCH_3$), 4.22–5.06 (m, 24H, $NCH_2N$, $NCH_2P$), 7.13–7.61 (m, 8H, Ar–H).

$^{13}$C{$^1$H}-NMR (75 MHz, $CH_3CN$-$d_3$, 298 K, ppm) $\delta$: 197.4, 190.1, 165.7, 162.8, 140.7, 138.7, 136.8, 129.5, 121.1, 79.6, 69.4, 65.3, 53.2, 52.7, 52.2, 46.7, 40.4, 17.4, 14.6.

$^{31}$P{$^1$H}-NMR (121 MHz, $CH_3CN$-$d_3$, 298 K, ppm) $\delta$: −38.9, −144.6 (sept, $J$ = 706.2 Hz, $PF_6^-$).

Elemental analysis calcd (%) for $C_{41}H_{53}ClF_{12}N_6O_{12}P_4Pd$: C, 37.43, H, 4.06, N, 6.39; found: C, 37.30, H, 4.12, N, 6.53.

**Synthesis of complex 7b.** To 0.0507 g (0.111 mmol) of palladium precursor **5** dissolved in 15 mL of anhydrous $CH_3CN$, 0.0608 g (0.204 mmol) of ligand **b** was added. The resulting solution was stirred for 30 min at room temperature. The solvent was removed under vacuum and the title complex was precipitated from a $CH_2Cl_2$/$Et_2O$ solution, filtered through a sintered glass filter, and dried under vacuum. 0.0939 g (yield 93%) of complex **7b** was obtained as a pale-yellow powder.

$^1$H NMR (300 MHz, $CH_3CN$-$d_3$, 298 K, ppm) $\delta$: 2.56 (s, 6H, $NCH_3$), 3.89–4.82 (m, 24H, $NCH_2N$, $NCH_2P$), 7.58 (d, $J$ = 8.7 Hz, Ar–H), 8.06 (d, $J$ = 8.7 Hz, Ar–H).

$^{13}$C{$^1$H}-NMR (75 MHz, $CH_3CN$-$d_3$, 298 K, ppm) $\delta$: 47.4 ($CH_2$, $PTA_{CH2}$), 49.0 ($CH_3$, $NCH_3$), 56.2 ($CH_2$, $PTA_{CH2}$), 68.9 ($CH_2$, $PTA_{CH2}$), 80.7 ($CH_2$, $PTA_{CH2}$), 122.6 (CH, Ar–CH), 136.7 (CH, Ar–CH), 146.4 (C, *p*-Ar–C), 157.1 (C, *i*-Ar–C).

$^{31}$P{$^1$H}-NMR (121 MHz, $CH_3CN$-$d_3$, 298 K, ppm) $\delta$: −50.8, −144.6 (sept, $J$ = 706.8 Hz, $PF_6^-$).

Elemental analysis calcd (%) for $C_{20}H_{34}F_{12}IN_7O_2P_4Pd$: C, 24.27, H, 3.46, N, 9.91; found: C, 24.50, H, 3.33, N, 9.99.

**Synthesis of complex 10b.** To 0.0462 g (0.126 mmol) of palladium precursor **9** dissolved in 10 mL of anhydrous $CH_3CN$, 0.0799 g (0.2519 mmol) of ligand **b** was added. The resulting solution was stirred for 30 min at room temperature. The solvent was removed under vacuum and the title complex was precipitated from a $CH_2Cl_2/Et_2O$ solution, filtered through a sintered glass filter, and dried under vacuum. 0.1179 g (yield 94%) of complex **10b** was obtained as a white powder.

$^1$H NMR (300 MHz, $CH_3CN$-$d_3$, 298 K, ppm) $\delta$: 2.17 (s, 3H, $NCH_3$), 3.28–3.62 (m, 1H, $H_{anti}$), 3.28–3.62 (m, 1H, $H_{anti}$), 4.02–5.01 (m, 12H, $NCH_2N$, $NCH_2P$), 4.36–4.61 (m, 1H, $H_{syn}$), 4.36–4.61 (m, 1H, $H_{syn}$), 5.45–5.60 (m, 1H, $H_{central}$).

$^{13}C\{^1H\}$-NMR (75 MHz, $CH_3CN$-$d_3$, 298 K, ppm) $\delta$: 80.9, 69.2, 56.0, 49.3, 47.3, 47.2.

$^{31}P\{^1H\}$-NMR (121 MHz, $CH_3CN$-$d_3$, 298 K, ppm) $\delta$: −39.2, −144.6 (sept, $J$ = 706.3 Hz, $PF_6^-$).

Elemental analysis calcd (%) for $C_{10}H_{20}ClF_6N_3P_2Pd$: C, 24.02, H, 4.03, N, 8.40; found: C, 23.85, H, 4.10, N, 8.52.

**Synthesis of complex 12b.** To 0.0405 g (0.0948 mmol) of palladium precursor **11** dissolved in 10 mL of anhydrous $CH_3CN$, 0.0897 g (0.205 mmol) of ligand **b** was added. The resulting solution was stirred for 30 min at room temperature. The solvent was removed under vacuum and the title complex was precipitated from a $CH_2Cl_2/Et_2O$ solution, filtered through a sintered glass filter, and dried under vacuum. 0.0822 g (yield 94%) of complex **12b** was obtained as a yellow powder.

$^1$H NMR (300 MHz, $CH_3CN$-$d_3$, 298 K, ppm) $\delta$: 2.18 (bs, 3H, $NCCH_3$) 2.21 (s, 3H, Ar–$CH_3$), 2.22 (s, 3H, Ar–$CH_3$), 2.68 (s, 6H, $NCH_3$), 4.02–4.99 (m, 24H, $NCH_2N$, $NCH_2P$) 7.02–7.43 (m, 3H, Ar–H).

$^{13}C\{^1H\}$-NMR (75 MHz, $CH_3CN$-$d_3$, 298 K, ppm) $\delta$: 172.8, 167.0, 140.4, 137.0, 130.0, 129.6, 128.3, 128.1, 125.6, 81.2, 68.5, 60.0, 59.3, 52.7, 51.9, 49.1, 18.0, 17.3, 14.8.

$^{31}P\{^1H\}$-NMR (121 MHz, $CH_3CN$-$d_3$, 298 K, ppm) $\delta$: −49.3, −144.5 (sept, $J$ = 708 Hz, $PF_6^-$).

Elemental analysis calcd (%) for $C_{24}H_{42}ClF_{12}N_7P_4Pd$: C, 31.25, H, 4.59, N, 10.63; found: C, 31.48, H, 4.37, N, 10.72.

**Synthesis of complex 14b.** To 0.0503 g (0.0764 mmol) of palladium precursor **13** dissolved in 30 mL of anhydrous $CH_3CN$, 0.0486 g (0.153 mmol) of ligand **b** was added. The resulting solution was stirred for 30 min at room temperature. The solvent was removed under vacuum and the title complex was precipitated from a $CH_2Cl_2/Et_2O$ solution, filtered through a sintered glass filter, and dried under vacuum. 0.0786 g (yield 99%) of complex **14b** was obtained as a white powder.

$^1$H NMR (300 MHz, $CH_3CN$-$d_3$, 298 K, ppm) $\delta$: 2.41 (s, 6H, Ar–$CH_3$), 2.77 (s, 6H, $NCH_3$), 3.92–4.25 (m, 2H, CH=CH), 4.14–5.02 (m, 24H, $NCH_2N$, $NCH_2P$), 7.04–7.11 (d, 4H, $J$ = 8.1 Hz, Ar–H), 7.30–7.38 (d, 4H, $J$ = 8.1 Hz, Ar–H).

$^{13}C\{^1H\}$-NMR (75 MHz, $CH_3CN$-$d_3$, 298 K, ppm) $\delta$: 143.6, 129.7, 126.3, 81.1, 69.4, 58.4, 49.6, 49.0, 20.7.

$^{31}P\{^1H\}$-NMR (121 MHz, $CH_3CN$-$d_3$, 298 K, ppm) $\delta$: −42.8, −144.6 (sept, $J$ = 706.7 Hz, $PF_6^-$).

Elemental analysis calcd (%) for $C_{30}H_{46}F_{12}N_6O_4P_4PdS_2$: C, 33.45, H, 4.30, N, 7.80; found: C, 33.70, H, 4.11, N, 7.89.

### Crystal structure determination

**7a** and **8a** crystals diffraction data were collected at XRD2 beamline of the Elettra Synchrotron, Trieste (Italy),[65] using a monochromatic wavelength of 0.620 Å, at 100 K. The data sets were integrated, scaled and corrected for Lorentz, absorption and polarization effects using XDS package.[66] The structures were solved by direct methods using SHELXT program[67] and refined using full-matrix least-squares implemented in SHELXL-2019/3.[68]

Thermal motions for all non-hydrogen atoms have been treated anisotropically and hydrogens have been included at calculated positions, riding on their carrier atoms. Geometric and thermal restraints (DFIX, DANG and SIMU) have been used to model disordered –$CF_3$ group in **8a.** The Coot program was used for structure building.[69] Pictures were prepared using Ortep3 (ref. 70) and Pymol[71] software.

Crystallographic data have been deposited at the Cambridge Crystallographic Data Centre and allocated deposition numbers CCDC 2411281 and 2411282, for **8a** and **7a** respectively.

### Cell viability assay

Cancer and non-cancerous cells were grown in agreement with the supplier and incubated at 37 °C (5% of $CO_2$). $1.5 \times 10^3$ cells were plated in 96 wells and treated with six different concentrations of palladium compounds (0.001, 0.01, 0.1, 1, 10, and 100 μM). These concentrations were achieved by diluting a DMSO stock solution of the complex (10 mM) in the culture medium. After 96 hours, cell viability was evaluated with CellTiter glow assay (Promega, Madison, WI, USA) with a Tecan M1000 instrument. $IC_{50}$ values were obtained from triplicates, and error bars are standard deviations.

### Computational details

The DNA blind docking studies were performed with AutoDock Vina 1.1.1 program,[72] using the B-DNA dodecamer crystallographic structure from the Protein Data Bank – PDB (ID 1BNA, sequence d(CGCGAATTCGCG)$_2$), according to previous studies.[73] The structures of the Pd ligand was obtained by full geometry optimization using the BLYP potential[74] combined with a Slater triple ζ quality basis set with two polarization functions with the small core approximation. Scalar relativistic effects were considered within the ZORA approximation.[75] This level of theory is denoted ZORA-BLYP/TZ2P and was chosen for the accurate results it can provide for compounds with heavy nuclei.[76] The DFT calculations were performed using ADF2019 (ref. 77) and provided also Hirshfeld partial charges that were used in the docking simulation. The DNA macromolecule was prepared using Chimera 1.8 software.[78] For intrinsic limits of the Autodock Vina software, the Pd atom was replaced by Zn for docking simulations, but it retained all the properties of this metal center obtained from the quantum mechanical results. An exhaustiveness of 50 was used, and the grid box was positioned in the center of the DNA structure (coordinates *xyz*: 14.75, 20.98, and 9.23; size: 50 × 50 × 50 Å).[49] As a model of the binding pose, we chose the ligand's conformer with the lowest

predicted binding free energy ($\Delta G$) from the most populated cluster.

## Data availability

The datasets supporting this article have been uploaded as part of the ESI.†

## Author contributions

Fabiano Visentin, Isabella Caligiuri, Flavio Rizzolio, Thomas Scattolin: conception and design of study; Tommaso Lorenzon, Maria Vescovo, Michele Maiullari, Giovanni Tonon, Nuno Reis Conceição, Martin C. Dietl, Nicola Demitri, Isabella Caligiuri, Pablo A. Nogara, Laura Orian, Thomas Scattolin: acquisition of data; Tommaso Lorenzon, Maria Vescovo, Michele Maiullari, Giovanni Tonon, Nuno Reis Conceição, Martin C. Dietl, Nicola Demitri, Abdallah G. Mahmoud, Isabella Caligiuri, Pablo A. Nogara, Laura Orian, Thomas Scattolin: analysis and/or interpretation of data; Thomas Scattolin, Fabiano Visentin, Pablo A. Nogara, Laura Orian, A. Stephen K. Hashmi, Flavio Rizzolio, Sónia A. C. Carabineiro: project management, fund acquisition, writing, reviewing, and editing.

## Conflicts of interest

There are no conflicts to declare.

## Acknowledgements

Centro de Química Estrutural (CQE) acknowledges the financial support of Fundação para a Ciência e Tecnologia (FCT) (projects UIDB/00100/2020, UIDP/00100/2020 and LA/P/0056/2020). FCT/MCTES is also acknowledged for projects UIDB/50006/2020 and UIDP/50006/2020 (LAQV) and bilateral project Portugal-Germany 5625-DRI-DAAD-2020/21. AGM acknowledges FCT for the international call of scientific employment stimulus (CEECIND, No. 2023.06724. CEECIND, DOI: **https://doi.org/10.54499/2023.06724.CEECIND/CP2836/CT0005**). This research was funded by Fondazione AIRC per la Ricerca sul Cancro, IG23566. TS and LO were supported by the Department of Chemical Sciences of the University of Padova [P-DiSC#01BIRD2024-UNIPD].

## Notes and references

1 A. D. Phillips, L. Gonsalvi, A. Romerosa, F. Vizza and M. Peruzzini, *Coord. Chem. Rev.*, 2004, **248**, 955–993.
2 J. Bravo, S. Bolaño, L. Gonsalvi and M. Peruzzini, *Coord. Chem. Rev.*, 2010, **254**, 555–607.
3 X. Tang, B. Zhang, Z. He, R. Gao and Z. He, *Adv. Synth. Catal.*, 2007, **349**, 2007–2017.
4 I. G. Shenderovich, *Molecules*, 2021, **26**, 1390.
5 S. N. Britvin and A. Lotnyk, *J. Am. Chem. Soc.*, 2015, **137**, 5526–5535.
6 S. N. Britvin, A. M. Rumyantsev, A. E. Zobnina and M. V. Padkina, *Chem.–Eur. J.*, 2016, **22**, 14227–14235.
7 D. A. Krogstad, J. Cho, A. J. DeBoer, J. A. Klitzke, W. R. Sanow, H. A. Williams and J. A. Halfen, *Inorg. Chim. Acta*, 2006, **359**, 136.
8 E. Vergara, S. Miranda, F. Mohr, E. Cerrada, E. R. T. Tiekink, P. Romero, A. Mendía and M. Laguna, *Eur. J. Inorg. Chem.*, 2007, 2926.
9 J. Spencer, A. Casini, O. Zava, R. P. Rathnam, S. K. Velhanda, M. Pfeffer, S. K. Callear, M. B. Hursthouseand and P. Dyson, *Dalton Trans.*, 2009, 10731.
10 J. Lasri, M. J. Fernández Rodríguez, M. F. C. Guedes da Silva, P. Smolenski, M. N. Kopylovich, J. J. R. Fraústo da Silva and A. J. L. Pombeiro, *J. Organomet. Chem.*, 2011, **696**, 3513.
11 M. Carreira, R. Calvo-Sanjuan, M. Sanauí, I. Marzo and M. Contel, *Organometallics*, 2012, **31**, 5772.
12 E. Guerrero, S. Miranda, S. Luüttenberg, N. Froöhlich, J. Koenen, F. Mohr, E. Cerrada, M. Laguna and A. Mendía, *Inorg. Chem.*, 2013, **52**, 6635.
13 J. Braddock-Wilking, S. Acharya and N. P. Rath, *Polyhedron*, 2014, **79**, 16; V. Ferretti, M. Fogagnolo, A. Marchi, L. Marvelli, F. Sforza and P. Bergamini, *Inorg. Chem.*, 2014, **53**, 4881.
14 R. Cortesi, C. Damiani, L. Ravani, L. Marvelli, E. Esposito, M. Drechsler, A. Pagnoni, P. Mariani, F. Sforza and P. Bergamini, *Int. J. Pharm.*, 2015, **492**, 291–300.
15 M. Porchia, F. Benetollo, F. Refosco, F. Tisato, C. Marzano and V. Gandin, *J. Inorg. Biochem.*, 2009, **103**, 1644–1651.
16 F. Scalambra, P. Lorenzo-Luis, I. De Los Ríos and A. Romerosa, *Eur. J. Inorg. Chem.*, 2019, **2019**, 1529–1538.
17 E. Atrián-Blasco, S. Gascón, M. J. Rodríguez-Yoldi, M. Laguna and E. Cerrada, *Eur. J. Inorg. Chem.*, 2016, **2016**, 2791–2803.
18 P. Bergamini, L. Marvelli, A. Marchi, V. Bertolasi, M. Fogagnolo, P. Formaglio and F. Sforza, *Inorg. Chim. Acta*, 2013, **398**, 11–18.
19 V. Ferretti, M. Fogagnolo, A. Marchi, L. Marvelli, F. Sforza and P. Bergamini, *Inorg. Chem.*, 2014, **53**, 4881–4890.
20 E. García-Moreno, S. Gascón, E. Atrián-Blasco, M. J. Rodriguez-Yoldi, E. Cerrada and M. Laguna, *Eur. J. Med. Chem.*, 2014, **79**, 164–172.
21 M. Sguizzato, R. Cortesi, E. Gallerani, M. Drechsler, L. Marvelli, P. Mariani, F. Carducci, R. Gavioli, E. Esposito and P. Bergamini, *Mater. Sci. Eng., C*, 2017, **74**, 357–364.
22 M. D. Živković, J. Kljun, T. Ilic-Tomic, A. Pavic, A. Veselinović, D. D. Manojlović, J. Nikodinovic-Runic and I. Turel, *Inorg. Chem. Front.*, 2018, **5**, 39–53.
23 C. Scolaro, A. Bergamo, L. Brescacin, R. Delfino, M. Cocchietto, G. Laurenczy, T. J. Geldbach, G. Sava and P. J. Dyson, *J. Med. Chem.*, 2005, **48**, 4161–4171.
24 K. J. Kilpin, S. M. Cammack, C. M. Clavel and P. J. Dyson, *Dalton Trans.*, 2013, **42**, 2008–2014.
25 A. Casini, G. Mastrobuoni, W. H. Ang, C. Gabbiani, G. Pieraccini, G. Moneti, P. J. Dyson and L. Messori, *ChemMedChem*, 2007, **2**, 631–635.
26 B. Dutta, C. Scolaro, R. Scopelliti, P. J. Dyson and K. Severin, *Organometallics*, 2008, **27**, 1355–1357.
27 M. Serrano-Ruiz, P. Lorenzo-Luis and A. Romerosa, *Inorg. Chim. Acta*, 2017, **455**, 528–534.

28 C. Gossens, A. Dorcier, P. J. Dyson and U. Rothlisberger, *Organometallics*, 2007, **26**, 3969–3975.
29 B. S. Murray, M. V. Babak, C. G. Hartinger and P. J. Dyson, *Coord. Chem. Rev.*, 2016, **306**, 86–114.
30 A. A. Nazarov, S. M. Meier, O. Zava, Y. N. Nosova, E. R. Milaeva, C. G. Hartinger and P. J. Dyson, *Dalton Trans.*, 2015, **44**, 3614–3623.
31 M. Rausch, P. J. Dyson and P. Nowak-Sliwinska, *Adv. Ther.*, 2019, **2**, 1900042.
32 R. H. Berndsen, A. Weiss, U. K. Abdul, T. J. Wong, P. Meraldi, A. W. Griffioen, P. J. Dyson and P. Nowak-Sliwinska, *Sci. Rep.*, 2017, **7**, 43005.
33 A. Weiss, R. H. Berndsen, M. Dubois, C. Müller, R. Schibli, A. W. Griffioen, P. J. Dyson and P. Nowak-Sliwinska, *Chem. Sci.*, 2014, **5**, 4742–4748.
34 S. Swaminathan and R. Karvembu, *ACS Pharmacol. Transl. Sci.*, 2023, **6**, 982–996.
35 S. Chatterjee, S. Kundu, A. Bhattacharyya, C. G. Hartinger and P. J. Dyson, *J. Biol. Inorg. Chem.*, 2008, **13**, 1149–1155.
36 T. Nhukeaw, K. Hongthong, P. J. Dyson and A. Ratanaphan, *Apoptosis*, 2019, **24**, 612–622.
37 R. F. S. Lee, S. Escrig, C. Maclachlan, G. W. Knott, A. Meibom, G. Sava and P. J. Dyson, *Int. J. Mol. Sci.*, 2017, **18**, 1869.
38 D. A. Wolters, M. Stefanopoulou, P. J. Dyson and M. Groessl, *Metallomics*, 2012, **4**, 1185.
39 T. Scattolin, E. Cavarzerani, D. Alessi, M. Mauceri, E. Botter, G. Tonon, I. Caligiuri, O. Repetto, U. Kamensek, S. K. Brezar, M. Dalla Pozza, S. Palazzolo, M. Cemazar, V. Canzonieri, N. Demitri, S. P. Nolan, G. Gasser, F. Visentin and F. Rizzolio, *Dalton Trans.*, 2025, **54**, 4685–4696.
40 T. Scattolin, E. Bortolamiol, F. Visentin, S. Palazzolo, I. Caligiuri, T. Perin, V. Canzonieri, N. Demitri, F. Rizzolio and A. Togni, *Chem.–Eur. J.*, 2020, **26**, 11868–11876.
41 T. Scattolin, N. Pangerc, I. Lampronti, C. Tupini, R. Gambari, L. Marvelli, F. Rizzolio, N. Demitri, L. Canovese and F. Visentin, *J. Organomet. Chem.*, 2019, **899**, 120857.
42 T. Scattolin, I. Caligiuri, L. Canovese, N. Demitri, R. Gambari, I. Lampronti, F. Rizzolio, C. Santo and F. Visentin, *Dalton Trans.*, 2018, **47**, 13616–13630.
43 J. Braddock-Wilking, S. Acharya and N. P. Rath, *Polyhedron*, 2014, **79**, 16–28.
44 J. Braddock-Wilking, S. Acharya and N. P. Rath, *Polyhedron*, 2015, **87**, 55–62.
45 T. Scattolin, S. Giust, P. Bergamini, I. Caligiuri, L. Canovese, N. Demitri, R. Gambari, I. Lampronti, F. Rizzolio and F. Visentin, *Appl. Organomet. Chem.*, 2019, **33**, e4902.
46 T. Scattolin, E. Bortolamiol, F. Rizzolio, N. Demitri and F. Visentin, *Appl. Organomet. Chem.*, 2020, **34**, e5876.
47 E. Bortolamiol, S. Novaselich, C. Tupini, S. Fagnani, R. Gambari, N. Demitri, I. Lampronti, F. Visentin and T. Scattolin, *Eur. J. Inorg. Chem.*, 2024, **27**, e202300673.
48 E. Bortolamiol, F. Visentin and T. Scattolin, *Appl. Sci.*, 2023, **13**, 5561.
49 G. Tonon, M. Mauceri, E. Cavarzerani, R. Piccolo, C. Santo, N. Demitri, L. Orian, P. A. Nogara, J. B. T. Rocha, V. Canzonieri, F. Rizzolio, F. Visentin and T. Scattolin, *Dalton Trans.*, 2024, **53**, 8463–8477.
50 T. Scattolin, V. A. Voloshkin, F. Visentin and S. P. Nolan, *Cell Rep. Phys. Sci.*, 2021, **2**, 100446.
51 E. J. Anthony, E. M. Bolitho, H. E. Bridgewater, O. W. L. Carter, J. M. Donnelly, C. Imberti, E. C. Lant, F. Lermyte, R. J. Needham, M. Palau, P. J. Sadler, H. Shi, F.-X. Wang, W.-Y. Zhang and Z. Zhang, *Chem. Sci.*, 2020, **11**, 12888–12917.
52 X. Xiong, L.-Y. Liu, Z.-W. Mao and T. Zou, *Coord. Chem. Rev.*, 2022, **453**, 214311.
53 G. Ferraro and A. Merlino, *Int. J. Mol. Sci.*, 2022, **23**, 3504.
54 A. T. Nies, H. Koepsell, K. Damme and M. Schwab, in *Handbook of Experimental Pharmacology*, 2010, pp. 105–167.
55 S. Spreckelmeyer, C. Orvig and A. Casini, *Molecules*, 2014, **19**, 15584–15610.
56 A. Mena-Cruz, P. Lorenzo-Luis, A. Romerosa, M. Saoud and M. Serrano-Ruiz, *Inorg. Chem.*, 2007, **46**, 6120–6128.
57 N. Reis Conceição, A. G. Mahmoud, M. F. C. Guedes da Silva, K. T. Mahmudov and A. J. L. Pombeiro, *Mol. Catal.*, 2023, **549**, 113512.
58 E. Atrián-Blasco, S. Gascón, M. J. Rodríguez-Yoldi, M. Laguna and E. Cerrada, *Eur. J. Inorg. Chem.*, 2016, **2016**, 2791–2803.
59 A. Madabeni, T. Scattolin, E. Bortolamiol, F. Visentin and L. Orian, *Organometallics*, 2024, **43**, 954–962.
60 T. Scattolin, I. Pessotto, E. Cavarzerani, V. Canzonieri, L. Orian, N. Demitri, C. Schmidt, A. Casini, E. Bortolamiol, F. Visentin, F. Rizzolio and S. P. Nolan, *Eur. J. Inorg. Chem.*, 2022, **2022**, e202200103.
61 T. Scattolin, G. Valente, L. Luzietti, M. Piva, N. Demitri, I. Lampronti, R. Gambari and F. Visentin, *Appl. Organomet. Chem.*, 2021, **35**, e6438.
62 L. Canovese, F. Visentin, G. Chessa, P. Uguagliati, C. Santo and A. Dolmella, *Organometallics*, 2005, **24**, 3297–3308.
63 M. Yamashita, J. V. Cuevas-Vicario and J. F. Hartwig, *J. Am. Chem. Soc.*, 2003, **125**, 16347.
64 D. Kruis, B. A. Markies, A. J. Canty, J. Boersma and G. Van Koten, *J. Organomet. Chem.*, 1997, **532**, 235.
65 A. Lausi, M. Polentarutti, S. Onesti, J. R. Plaisier, E. Busetto, G. Bais, L. Barba, A. Cassetta, G. Campi, D. Lamba, A. Pifferi, S. C. Mande, D. D. Sarma, S. M. Sharma and G. Paolucci, *Eur. Phys. J. Plus*, 2015, **130**, 1.
66 W. Kabsch, *Acta Crystallogr., Sect. D: Biol. Crystallogr.*, 2010, **66**, 125.
67 G. M. Sheldrick, *Acta Crystallogr., Sect. A*, 2015, **71**, 3.
68 G. M. Sheldrick, *Acta Crystallogr., Sect. C:Struct. Chem.*, 2015, **71**, 3.
69 P. Emsley, B. Lohkamp, W. Scott and K. Cowtan, *Acta Crystallogr., Sect. D:Biol. Crystallogr.*, 2010, **66**, 486.
70 L. Farrugia, *J. Appl. Crystallogr.*, 2012, **45**, 849.
71 L. Schrodinger, 2015, **http://www.pymol.org**.
72 O. Trott and A. J. Olson, *J. Comput. Chem.*, 2009, **31**, 455.
73 (*a*) R. A. Hussain, A. Badshah, M. Sohail, B. Lal and K. Akbar, *J. Mol. Struct.*, 2013, **1048**, 367; (*b*) A. Zianna, G. D. Geromichalos, A.-M. Fiotaki, A. G. Hatzidimitriou, S. Kalogiannis and G. Psomas, *Pharmaceuticals*, 2022, **15**,

886; (*c*) N. Shahabadi, L. Ghaffari, Z. Mardani and F. Shiri, *Biol. Trace Elem. Res.*, 2021, **200**, 1988–2000.

74 (*a*) C. Lee, W. Yang and R. G. Parr, *Phys. Rev. B: Condens. Matter Mater. Phys.*, 1988, **37**, 785; (*b*) A. D. Becke, *Phys. Rev. A*, 1988, **38**, 3098.

75 E. van Lenthe, E. J. Baerends and J. G. Snijders, *J. Chem. Phys.*, 1994, **101**, 9783.

76 (*a*) M. Bortoli, S. M. Ahmad, T. A. Hamlin, F. M. Bickelhaupt and L. Orian, *Phys. Chem. Chem. Phys.*, 2018, **20**, 27592; (*b*) M. Dalla Tiezza, F. M. Bickelhaupt and L. Orian, *ChemistryOpen*, 2019, **8**, 143; (*c*) M. Dalla Tiezza, F. M. Bickelhaupt and L. Orian, *ChemPhysChem*, 2018, **19**, 1766; (*d*) L. Orian, L. P. Wolters and F. M. Bickelhaupt, *Chem.–Eur. J.*, 2013, **40**, 12227; (*e*) L. Orian, M. Swart and F. M. Bickelhaupt, *ChemPhysChem*, 2014, **15**, 219; (*f*) A. Madabeni, M. Bortoli, P. A. Nogara, J. B. T. Rocha and L. Orian, *Inorg. Chem.*, 2021, **60**, 4646; (*g*) L. Orian, W.-J. van Zeist and F. M. Bickelhaupt, *Organometallics*, 2008, **27**, 4028.

77 (*a*) E. J. Baerends, D. E. Ellis and P. Ros, *Chem. Phys.*, 1973, **2**, 41; (*b*) G. te Velde, F. M. Bickelhaupt, E. J. Baerends, C. F. Guerra, S. J. A. van Gisbergen, J. G. Snijders and T. Ziegler, *J. Comput. Chem.*, 2001, **22**, 931.

78 (*a*) E. F. Pettersen, T. D. Goddard, C. C. Huang, G. S. Couch, D. M. Greenblatt, E. C. Meng and T. E. Ferrin, *J. Comput. Chem.*, 2004, **25**, 1605; (*b*) P. A. Nogara, F. B. Omage, G. R. Bolzan, C. P. Delgado, L. Orian and J. B. T. Da Rocha, *J. Mol. Model.*, 2022, **28**, 354.